Electronic Supplementary Material (ESI) for Journal of Materials Chemistry C.

Supporting Information

Recognition Mechanism of Molecularly Imprinted Polymers by Aggregation-Induced Emission

Yuwei Wu †, Jiang Liu †, Wenbin Huang, Zikai He*, Jia Zhou*, Yingchun Li*

School of Science, Harbin Institute of Technology, Shenzhen, 518055, China

† The authors contributed equally to this work

* Corresponding authors

Yingchun Li
E-mail address: liyingchun@hit.edu.cn
Tel/Fax: +86-755-86239466

Jia Zhou
E-mail address: jiajoe@gmail.com

Zikai He
E-mail address: hezikai@hit.edu.cn

Tel/Fax: +86-0755-86134233

** Correspondence to: Y. Li, School of Science, Harbin Institute of Technology, Shenzhen, 518055, China.

Table of contents

Captions

Figure S1 Scheme of the synthetic route of TPE-Ph.

Figure S2 1H NMR spectrum of TPE-Ph in $CDCl_3$.

Figure S3 SEM images of TPE-Ph-MIP, NIP-2.

Figure S4 Surface area and total porous volumes of TPE-Ph-MIP and NIP-2.

Figure S5 Infrared spectra of template molecule, TPE-Ph-MIP before and after template extraction. Insets are photographs of TPE-Ph-MIP before and after template elution, which were taken under illumination of a UV lamp.

Figure S6 Isothermal adsorption model of Langmuir and Freundlich of TPE-2NH_2-MIP in sorption of TPE-2NH_2.

Figure S7 Isothermal adsorption model of Langmuir and Freundlich of TPE-Ph-MIP in sorption of TPE-Ph.

Figure S8 Scatchard plot of TPE-2NH_2-MIP sorbing TPE-2NH_2.

Figure S9 Scatchard plot of TPE-Ph-MIP sorbing TPE-Ph.

Figure S10 Molecular simulation model of TPE-4NH_2 and MAA at minimize energy. (O: red; H: white; N: blue; C in TPE-4NH_2: gray; C in MAA: yellow)

Figure S11 Molecular simulation model of TPE-COOH and styrene at minimize energy. (O: red; H: white; C in TPE-COOH: gray; C in styrene: yellow)

Figure S12 Standard curves of TPE, TPE-2NH_2, TPE-4NH_2, TPE-Ph and TPE-COOH obtained by UV-vis spectrometry.

Figure S13 The fluorescence spectra of TPE-MIP-1, TPE-2NH_2-MIP, TPE-4NH_2-MIP, NIP-1, TPE-MIP-2, TPE-Ph-MIP, TPE-COOH-MIP, NIP-2 and TPE mixed with TPE-2NH_2-MIP at the content ratio of 1% (wt%).

Figure S14 Calibration curves of TPE (A), TPE-2NH_2 (B) and TPE-4NH2 (C) sorbed by TPE-2NH$_2$-MIP; TPE (D), TPE-Ph (E) and TPE-COOH (F) sorbed by TPE-COOH-MIP based on solid-state fluoremetry.

Table S1 Composition of polymerization recipes.

Table S2 Imprinting factor (α) of polymers interacting with substrate molecules.

Table S3 Comparison between the methods of UV-vis and solid fluorescence spectrometry.

1 Instruments and reagents

4-[2-(4-aminophenyl)-1,2-diphenylethenyl] aniline (TPE-$2NH_2$), 1,1,2,2-Tetrakis (4-aminophenyl) ethene (TPE-$4NH_2$) and 1,1,2,2-Tetra (4-carboxylbiphenyl) ethylene (TPE-COOH) were purchased from HWRK chemical (Beijing, China; www.hwrkchemical.com). 1,2-diphenyl-1,2-bis(4-phenylphenyl) ethene (TPE-Ph) was synthesized and the detailed procedure was given in the supporting information (Figure S1). Tetraphenylethylene (TPE) and the initiator 2, 2'-Azobis (isobutyronitrile) (AIBN) were bought from TCI (Shanghai, China; www.tcichemicals.com). Styrene, methacrylic acid (MAA) and divinylbenzene (DVB) were obtained from Alfa Aesar (Shanghai, China; www.alfa.com). Acetone, tetrahydrofuran (THF), methyl alcohol and glacial acetic acid were purchased from Adamas Reagent Co. Ltd. (Shanghai, China; www. adamas-beta.com). THF was of spectroscopic level and the rest are of analytical grade.

Preparation of polymers was carried out in a thermostat water bath (XMTD-702). UV-vis spectrometer (SHIMADSZU UV-2600) was used to measure the concentration of substrate molecules before and after adsorption. Fluorescence intensity was measured with a fluorescence spectrometer (HORIBA FluoroMax-4). Fluorescence photographs were obtained by using a Canon camera (EOS 800D).

2 Synthesis of TPE-Ph

A 150 mL flask was charged with Phenyl *p*-biphenylyl ketone (2.58 g, 10 mmol), Zn (1.96 g, 30 mmol) under nitrogen atmosphere. 80 mL anhydrous THF was injected into the flask and the resulting mixture was maintaining −10 ℃ for 20 min then to slowly injecting TiCl$_4$ 1.65 mL (2.85 g, 15 mmol) into the solution under stirring for 10 min. Subsequently, the solvent was maintaining room temperature for 30 min then to refluxing for 6 hours. After reaction finished, the resulting solvent was maintained at room temperature and quenched with 1 N saturated K$_2$CO$_3$ solution. Afterwards, the solvent was filtrated and the filter liquor was extracted with dichloromethane and saturated NH$_4$Cl. After the solvent was removed by rotary evaporation, the residue was purified by flash column chromatography (silica gel, petroleum ether/ CH$_2$Cl$_2$ = 5:1) to give product (1.4425 g, 59.5 %) as a white solid. ^{1}H NMR (600 MHz, CDCl$_3$) (ppm): 7.58-7.54 (m, 4H), 7.42-7.34 (m, 8H), 7.32-7.28 (m, 2H) , 7.26-7.08 (m, 14H).

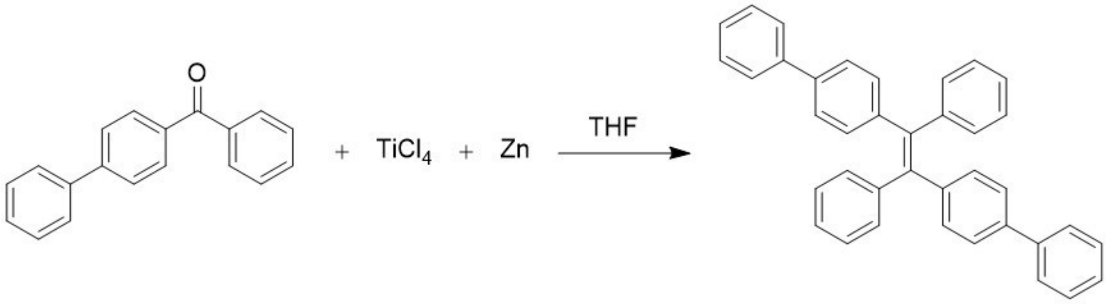

Figure S1 Scheme of the synthetic route of TPE-Ph.

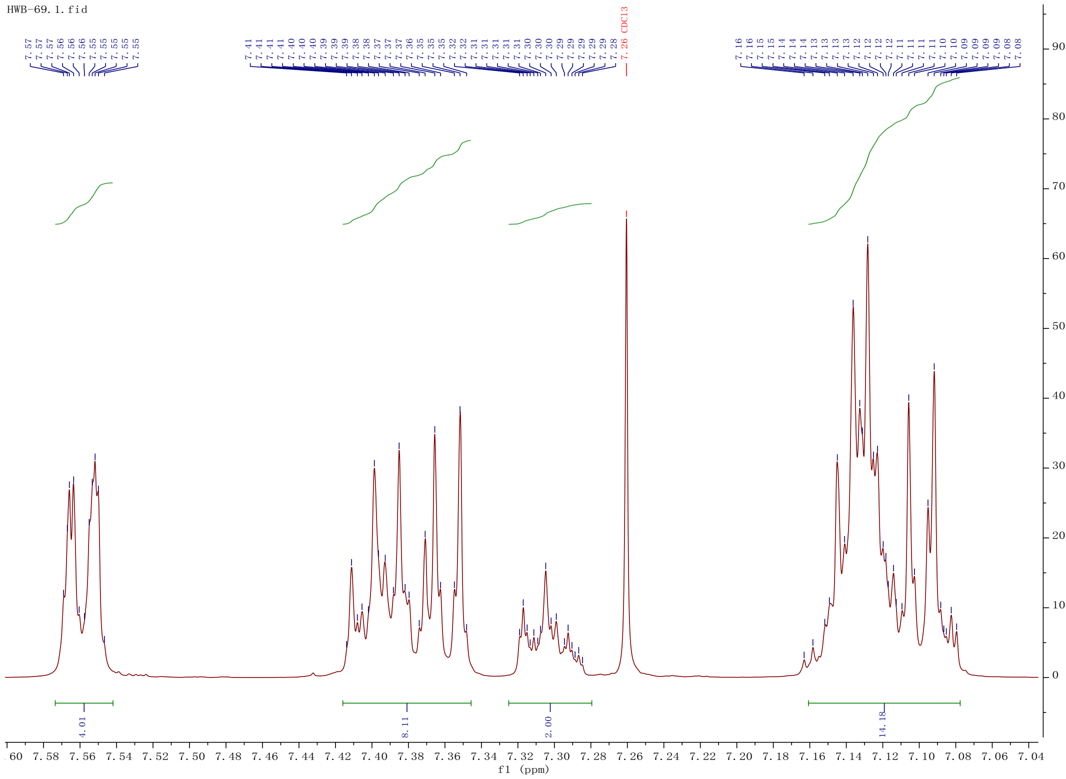

Figure S2 ^{1}H NMR spectrum of TPE-Ph in $CDCl_3$.

3 Adsorption experiment

General operation of sorption and calculation of sorbing capacity: The required mass of polymers (60 mg) was weighed into a 5 mL screw-cap vial. 3.5 mL of substrate solution in THF was added, and the vial was sealed and placed in a shaker. Except in the kinetics experiments, samples were shaking overnight at room temperature to allow binding equilibrium. Afterwards, the mixture was centrifuged at 4500 rpm for 10 min, and the supernatant solution was analyzed by UV-vis to determine the concentration of substrate molecules. According to the changes of the amount of substrate before and after adsorption, the equilibrium adsorption capacity factor (Q, μmol/g) was calculated.

$$Q=\frac{(C_0-C_t)\mathrm{V}}{\mathrm{m}} \qquad （1）$$

where C_0 is the initial molecular concentration (μmol/mL); C_t is the molecular concentration of the supernatant (μmol/mL); V is the molecular solution volume (mL); and m is the mass of polymer (g).

(1) Isothermal adsorption experiment

For static adsorption experiment of FG effect, a certain mass of TPE-2NH$_2$-MIP and NIP-1 were respectively added into the solutions of TPE, TPE-2NH$_2$ and TPE-4NH$_2$ at the concentration range of 1~50 mM. As for that of size effect, TPE-Ph-MIP were mixed in TPE, TPE-Ph and TPE-COOH solutions at the concentration of 1~40 mM.

(2) Maximum adsorption experiment

For FG effect, the required amount of TPE-MIP-1, TPE-2NH$_2$-MIP, TPE-4NH$_2$-MIP and NIP-1 were separately weighted in screw-cap vials containing the solution of TPE, TPE-2NH$_2$ and TPE-4NH$_2$ at the concentration of 50 mM. The following adsorption experiments and calculation of the maximum adsorption capacity (Q_m) were performed according to the above-described general operation. For size effect, the polymers were TPE-MIP-2, TPE-Ph-MIP, TPE-COOH-MIP and NIP-2, and the sorption experiments took place in 40 mM TPE, TPE-Ph and TPE-COOH.

(3) Dynamic adsorption experiment

For FG effect, the required amount of TPE-2NH$_2$-MIP and NIP-1 were weighed in screw-cap vials containing 50-mM TPE-2NH$_2$ solution. After sorption for a certain period of time (5, 10, 20, 30, 60, 90, 120, 150, 180, 240, 300, 360 min), the supernatant solution was analyzed by UV-vis. Investigation of size effect was nearly the same as FG effect, except that the polymers were TPE-Ph-MIP and NIP-2, and the sorption took place in 40 mM TPE-Ph.

4 Morphological and structural characterization

For size effect, TPE-Ph-MIP and NIP-2 were selected for characterization. In Figure S3, the SEM images of TPE-Ph-MIP and NIP-2 also shows that the structure of both polymers are porous.

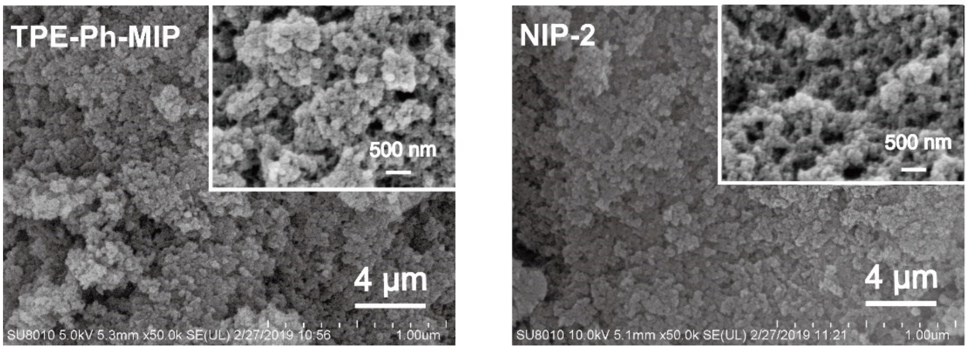

Figure S3 SEM images of TPE-Ph-MIP and NIP-2.

As similarly with Figure 2B, in Figure S4, the specific surface area and the total pore volume of TPE-Ph-MIP are both larger than NIP-2, which can be more conducive to the mass transportation of substrate molecules.

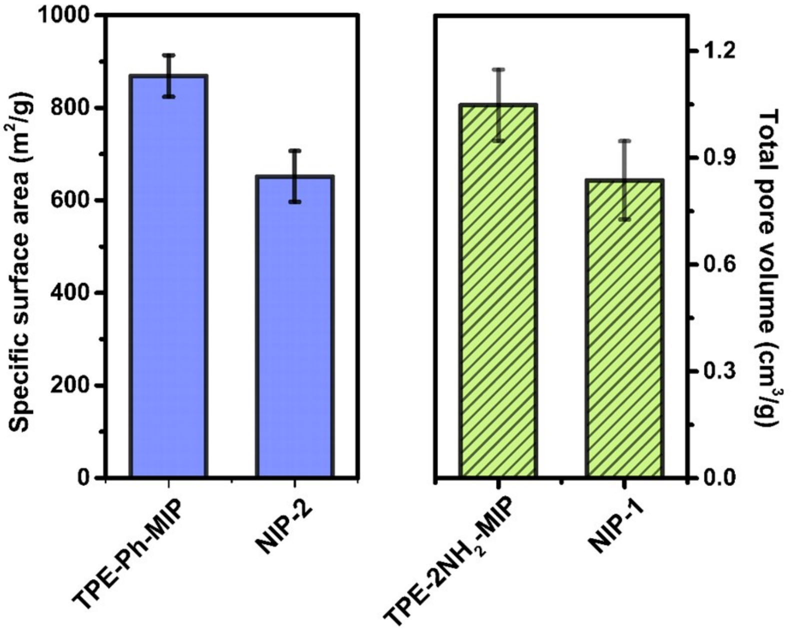

Figure S4 Surface area and total porous volumes of TPE-Ph-MIP and NIP-2.

For TPE-Ph-MIP, the absorption peak at 761 cm^{-1} arises from the out-of-plane deformation vibration of C−H in the monosubstituted aromatic ring of TPE-Ph molecule. Besides, the peaks at 824 cm^{-1} can be ascribed to the para-substituted benzene ring of DVB in polymer (curve b and c). After template extraction, the above peaks corresponding to TPE-Ph almost disappeared and only the peaks belonging to DVB retained, demonstrating that TPE-Ph molecules were removed from MIP skeleton.

It is worth nothing that, under UV irradiation, TPE-Ph-MIP have distinct fluorescence before template extraction, while the fluorescence density was attenuated significantly after elution. However, there was still dim fluorescent in TPE-Ph-MIP and the enlarged view of that was obtained in the inset of Figure S5. The issue of template leakage can be confirmed in visualization.

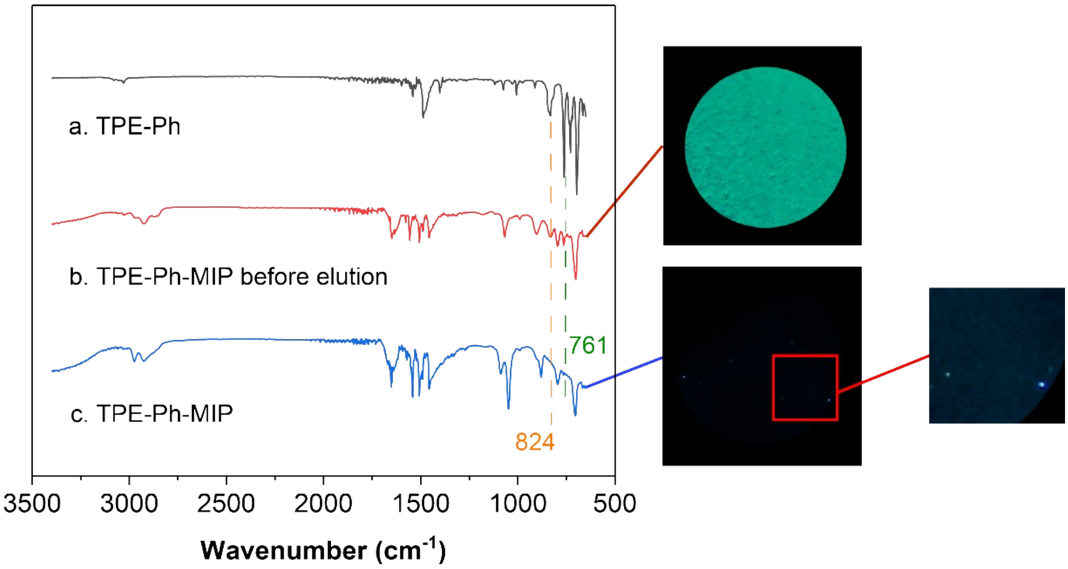

Figure S5 Infrared spectra of template molecule (curve a), TPE-Ph-MIP before (curve b) and after (curve c) template extraction. Insets are the corresponding photographs of polymers, which were taken under illumination of a UV lamp.

5 Fitting of mathematical models

(1) The adsorption models of Langmuir and Freundlich

Langmuir and Freundlich, whose equations are expressed as:

$$\frac{C_{\mathrm{e}}}{Q_{\mathrm{e}}}=\frac{C_{\mathrm{e}}}{Q_{\mathrm{m}}}+\frac{1}{\mathrm{K_L}Q_{\mathrm{m}}} \quad (2)$$

$$\lg Q_{\mathrm{e}}=\frac{1}{\mathrm{K_F}}Q_{\mathrm{e}}+\lg Q_{\mathrm{m}} \quad (3)$$

where Q_{m} is the maximum adsorption capacity; $\mathrm{K_L}$ and $\mathrm{K_F}$ are the Langmuir and Freundlich adsorption equilibrium constant.

Fitting results were given in Figure S8 and FigureS9.

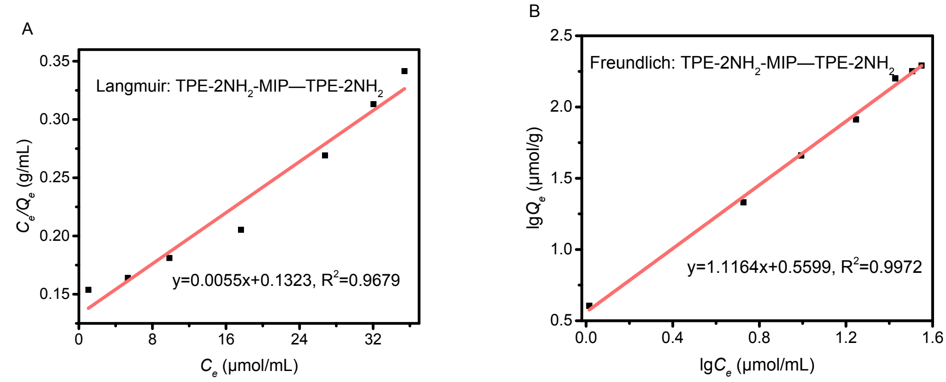

Figure S6 Isothermal adsorption model of Langmuir (A) and Freundlich (B) of TPE-2NH$_2$-MIP in sorption of TPE-2NH$_2$.

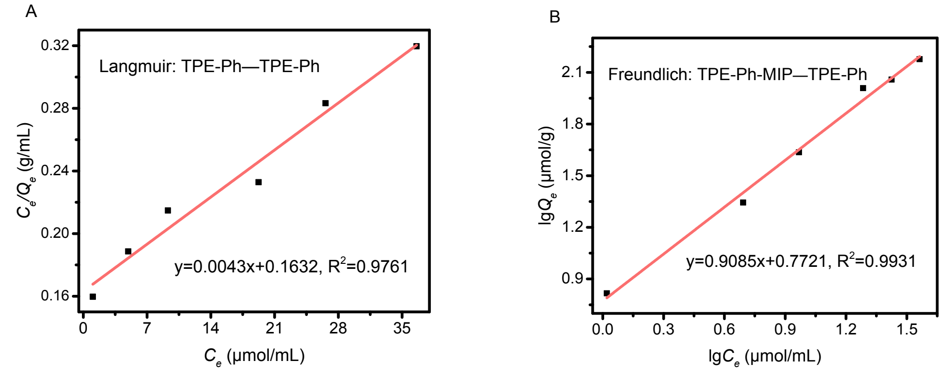

Figure S7 Isothermal adsorption model of Langmuir (A) and Freundlich (B) of TPE-Ph-MIP in sorption of TPE-Ph.

(2) Scatchard analysis

Scatchard equation is expressed as follows:

$$\frac{Q_e}{C_e} = \frac{Q_m - Q_e}{K_d} \quad (4)$$

where K_d is the equilibrium dissociation constant (μmol/mL) and the rest parameters are the same as denoted above.

Fitting results were presented in Figure S10 and FigureS9.

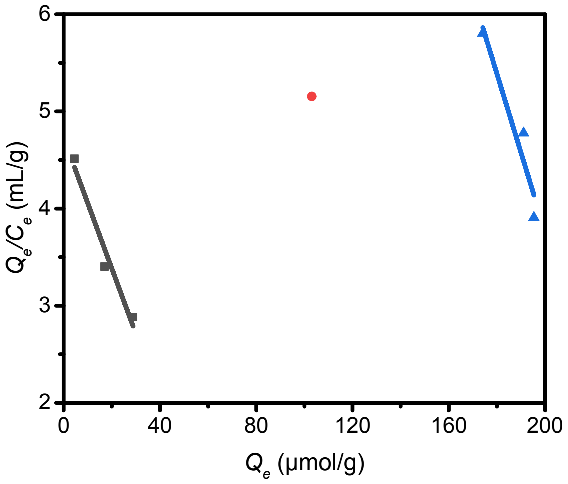

Figure S8 Scatchard plot of TPE-2NH$_2$-MIP sorbing TPE-2NH$_2$.

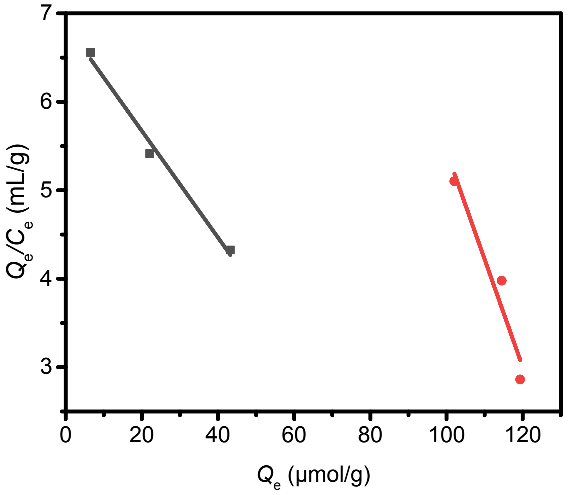

Figure S9 Scatchard plot of TPE-Ph-MIP sorbing TPE-Ph.

6 Imprinting factors

Table S2 Imprinting factors (*α*) of polymers interacting with substrate molecules.

FG effect				**Size effect**			
Substrates	TPE-MIP-1	TPE-2NH$_2$-MIP	TPE-4NH$_2$-MIP	**Substrates**	TPE-MIP-2	TPE-Ph-MIP	TPE-COOH-MIP
TPE	**1.66**	1.72	2.15	TPE	**3.93**	4.14	5.11
TPE-2NH$_2$	1.57	**2.63**	2.98	TPE-Ph	3.77	**6.35**	7.74
TPE-4NH$_2$	1.64	2.61	**3.14**	TPE-COOH	2.63	6.03	**11.77**

7 Computational details

All computations were carried out with the Gaussian09 program[1]. All of the geometries were fully optimized by B97D3 functional[2] with the D95(d,p) basis set unless noted otherwise. The final interaction energy between polymers and templates was calculated by B97D3/6-311+G(d,p) level of theory. In order to remove the basis set superposition error (BSSE) from the value of interaction energy, the counterpoise correction by Boys and Bernardi[3] was employed. Because the ratio between the template molecules and functional monomers in polymers is roughly one to four in the experiments, we chose the same ratio in our calculations assuming this would be the most likely configuration. Our current model is undoubtedly a simplified model because there would be various configurations with different ratios for template molecules and functional monomers in polymers in the real experiments. However, it is a feasible choice balancing the accuracy and computational cost. Once the functional monomers reach the optimal position with the template molecules, they are kept fixed during the optimization with other substrate molecules.

Figure S12 and S13 are figures of simulation model when template molecules TAPE and TCBE respectively interact with their functional monomers and reach the most stable state. The atom C of templates and functional monomers are distinguished by different colors to observe clearly. Respectively, gray was used in template molecules while yellow was used in monomers.

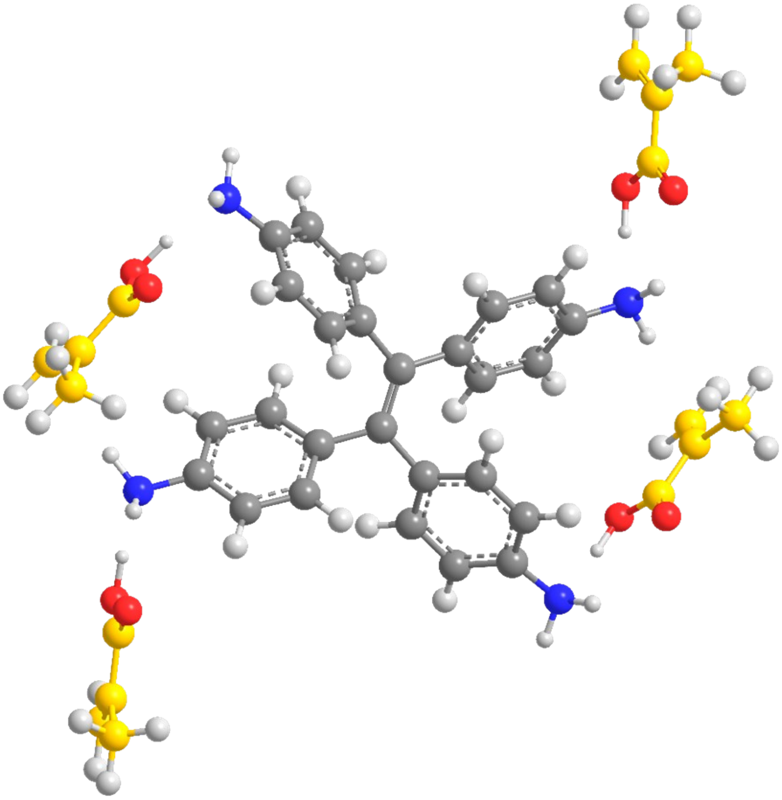

Figure S10 Molecular simulation model of TPE-4NH$_2$ and MAA at minimize energy. (O: red; H: white; N: blue; C in TPE-4NH$_2$: gray; C in MAA: yellow)

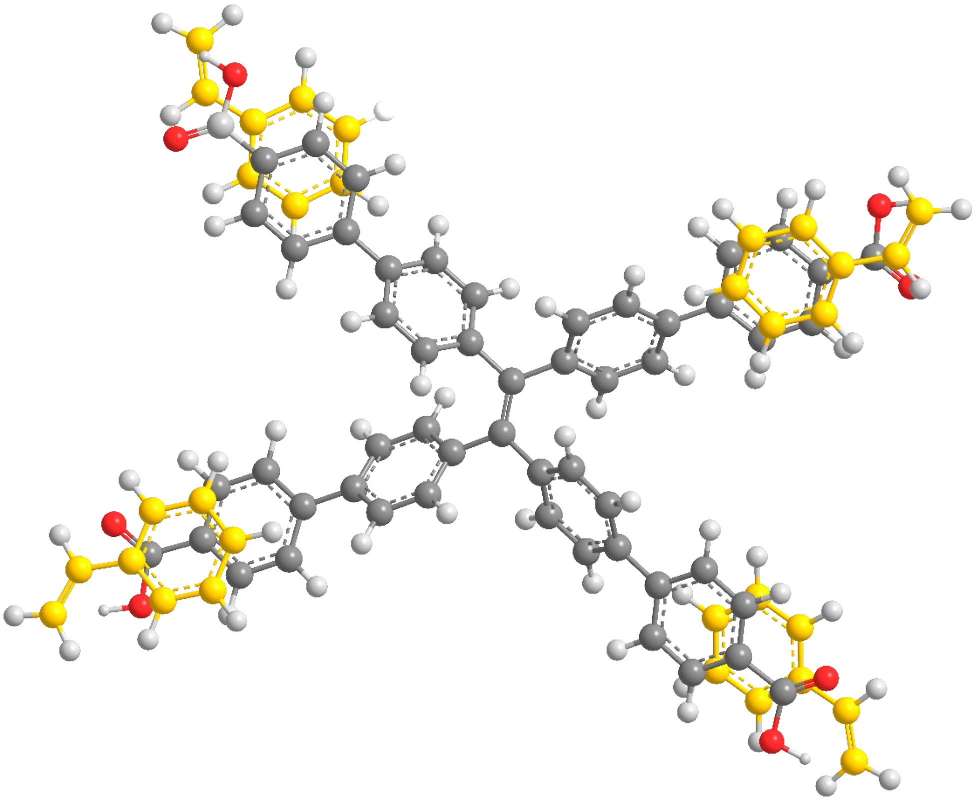

Figure S11 Molecular simulation model of TPE-COOH and styrene at minimize energy. (O: red; H: white; C in TPE-COOH: gray; C in styrene: yellow)

8 Analysis by UV-vis and solid state fluorescence spectrometry

(1) UV-vis spectrometry

Quantification of sorption capacity of polymers is usually carried out in an indirect manner by measuring the concentration changes of substrate molecules in the supernatant before and after sorption. In this work, UV-vis spectrometry was employed to do the detection, and the standard curves of substrate molecules are shown in Figure S12.

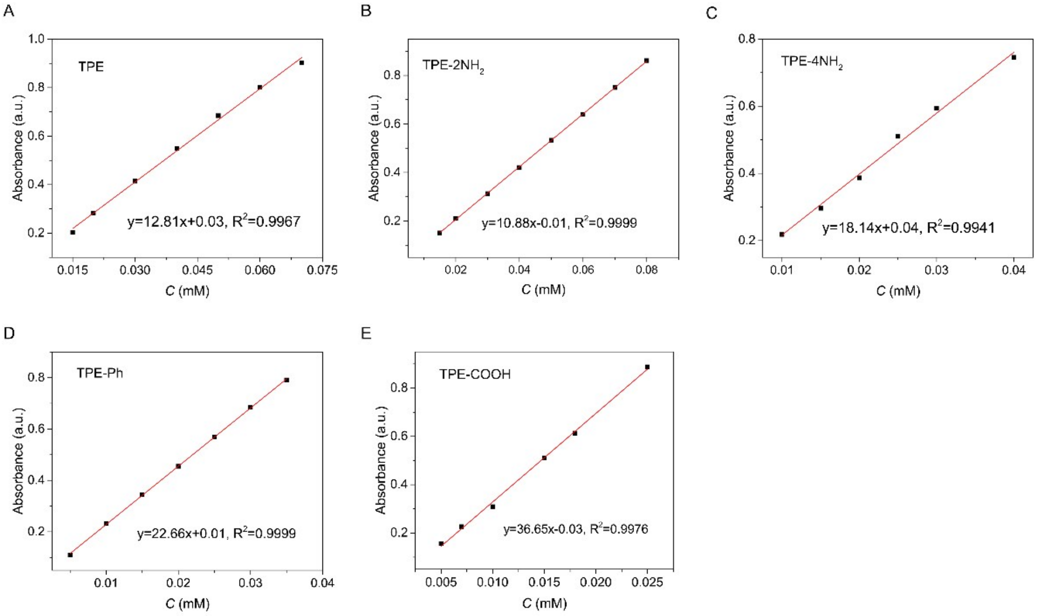

Figure S12 Standard curves of TPE (A), TPE-2NH$_2$ (B), TPE-4NH$_2$ (C), TPE-Ph (D) and TPE-COOH (E) obtained by UV-vis spectrometry.

(2) Solid state fluorescence spectrometry

Due to imprinting and AIE effects, the molecules were immobilized in cavities after being adsorbed by polymers and subsequently emit fluorescence. For this reason, a method of solid-state fluorescence was established and can directly obtain the adsorption capacity by detecting the fluorescence intensity of polymers.

First, the required amounts of polymers (TPE-2NH$_2$-MIP, NIP-1, TPE-Ph-MIP and NIP-2) were weighed in screw-cap vials containing a range of AIEgen solutions. After reaching adsorption equilibrium, the AIEgens in supernatant solution were analyzed by UV-vis and the amount of AIEgens sorbed by polymers (Q) were calculated by subtracting from the total amount. Fluorescence intensity of polymers after adsorption was measured by spectrometer, and the standard curves of solid-state fluorescence were established between intensity and *Q*. Figure S13 shows that all the eight polymers (TPE-MIP-1, TPE-2NH$_2$-MIP, TPE-4NH$_2$-MIP, NIP-1, TPE-MIP-2, TPE-Ph-MIP, TPE-COOH-MIP and NIP-2) present similar fluorescent spectra and their fluorescent signals are far weaker than that of TPE at a low content ratio. Thus, the fluorescence intensity of the polymers themselves can be ignored in the calculation. The calibration curves for the solid-state fluorometry were then built up (Figure S14A~F).

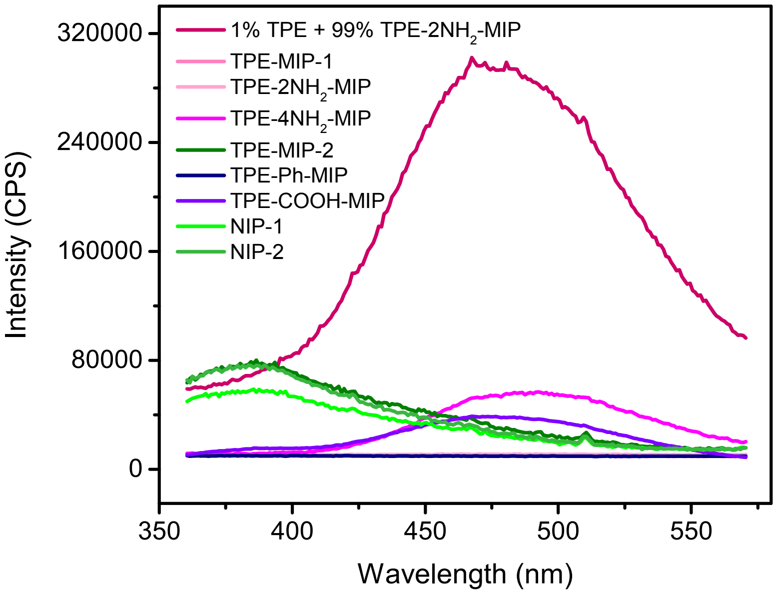

Figure S13 The fluorescence spectra of TPE-MIP-1, TPE-2NH$_2$-MIP, TPE-4NH$_2$-MIP, NIP-1, TPE-MIP-2, TPE-Ph-MIP, TPE-COOH-MIP, NIP-2 and TPE mixed with TPE-2NH$_2$-MIP at the content ratio of 1% (wt%).

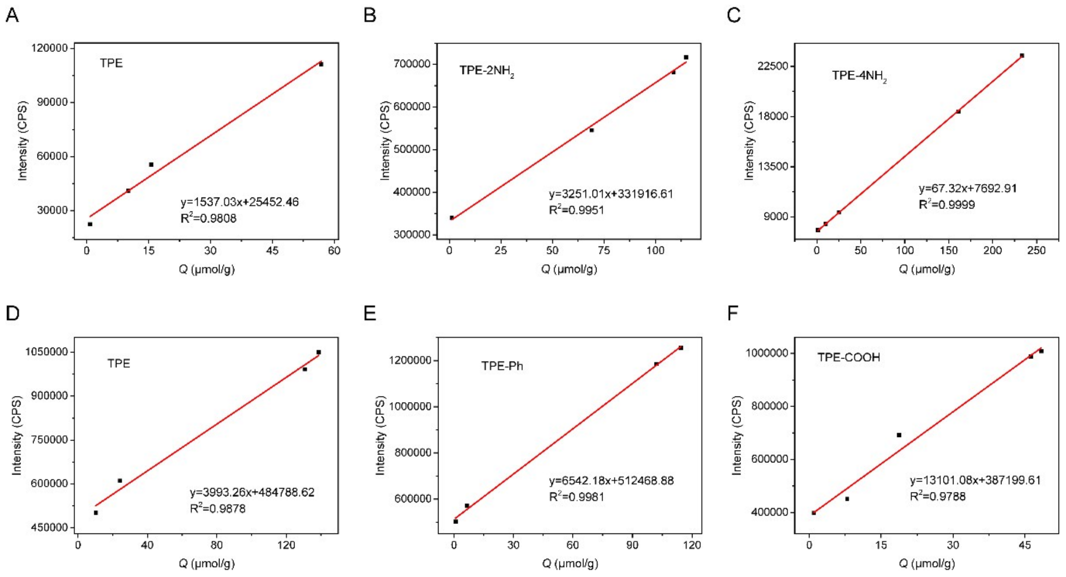

Figure S14 Calibration curves of TPE (A), TPE-$2NH_2$ (B) and TPE-$4NH_2$ (C) sorbed by TPE-$2NH_2$-MIP; TPE (D), TPE-Ph (E) and TPE-COOH (F) sorbed by TPE-COOH-MIP based on solid-state fluoremetry.

(3) Comparison of analytical methods based on UV-vis and solid state fluorescence spectrometry

UV-vis spectrometry is an indirect way by comparing concentration changes of substrate in the supernatant before and after sorption, while solid state fluorescence method can directly obtain the adsorption capacity by measuring the fluorescence intensity of polymers. As presented in Figure S14 and Figure S12, they differ in detection range. The linear range of all the AIEgens measured by solid state fluorescence spectrometry cover Q_m values of polymers in experiments. However, for UV-vis spectrometry, the linear range is very limited. This can be attributed to the shortcoming of absorption spectrometry, since absorbance located in the range of 0.2-0.8 is the prerequisite of the Lambert-Beer law. In addition, solid fluorescence standard specimens can be stored for a long term, while standard solutions for UV-vis spectrometry are unable to last long. In conclusion, the method of fluorescence also has advantages of easy operation, large linear range, reusability of standard fluorescent specimens, etc. Nonetheless, the Q values obtained by UV-vis and fluorescence spectrometry still have slight differences, and we believe further optimization and calibration will bring about comparable results.

Table S3 Comparison of analytical methods based on UV-vis and solid state fluorescence spectrometry.

Methods	UV-vis spectrometry	Solid state fluorescence spectrometry
Applicability of Analyte	High	Low
Sensitivity	Low	High
Linear range	Narrow	Wide
Establishment of standard curve	Using standard solutions and suffering short-time storage	Using standard solid specimens and having long-time storage
Operation	Indirect and complex	Direct and easy

References

1. M. Frisch, G. Trucks, H. B. Schlegel, Gaussian 09, revision a. 02, gaussian, *Inc., Wallingford, CT,* 2009, **200**, 28.
2. S. Grimme, S. Ehrlich and L. Goerigk, Effect of the damping function in dispersion corrected density functional theory, *Journal of computational chemistry,* 2011, **32 (7)**, 1456-1465.
3. S. F. Boys and F. d. Bernardi, The calculation of small molecular interactions by the differences of separate total energies. Some procedures with reduced errors, *Molecular Physics,* 1970, **19 (4)**, 553-566.